The Magnetic and Velocity Fields of Solar Active Regions
ASP Conference Series, Vol. 46, 1993
Harold Zirin, Guoxiang Ai, and Haimin Wang (eds.)

FORMATION OF SOLAR PROMINENCES WITH NORMAL AND INVERSE POLARITIES

G. S. CHOE and L. C. LEE

Geophysical Institute, University of Alaska
Fairbanks, AK 99775-0800, U.S.A.

ABSTRACT Numerical simulations of solar prominence formation are presented employing photospheric horizontal motions as boundary conditions. Three different combinations of magnetic field configurations and footpoint motions are considered: (1) a bipolar arcade with a footpoint shear, (2) an arcade exposed to a shearing and converging motion, (3) two adjacent arcades undergoing a shearing and converging motion. In each case, it is found that the dynamic evolution of magnetic fields can force the plasma into a thermal instability leading to the formation of a prominence.

1. INTRODUCTION

It is well known that solar prominences are supported by magnetic fields against gravity. The prototype static models by Kippenhahn & Schlüter (1957) and Kuperus & Raadu (1974) represent two different field topologies or *polarities* of prominences. In the normal polarity prominences, the direction of the magnetic field normal to the prominence plane is parallel to that of the plausible ambient field while it is reversed in the inverse polarity prominences.

Prominences are always located above magnetic neutral lines, along which the photospheric magnetic fields and chromospheric fibrils are highly aligned (Martin 1990). Rompolt & Bogdan (1986) observed that shearing mass motions and converging motions towards the neutral line lead to prominence formation. The cancellation of opposite fluxes on the neutral line seen in magnetograms also indicates the existence of converging flows and further implies the reconnection of field lines either above or below the photosphere. A helmet-shaped arcade observed over a prominence sometimes surrounds more than one bipolar regions, and a survey by Tang (1987) showed that more prominences are formed between bipolar regions than inside one bipolar region.

Based on these observations, we investigate the evolution of the coronal plasma with magnetic arcades imposing shearing and converging photospheric motions as physical boundary conditions. Initially we assume an isothermal hydrostatic atmosphere with a potential field which is either bipolar (Cases A and B) or quadrupolar (Case C). Then we numerically solve the two-dimensional time-dependent compressible MHD equations including the

gravity, field-aligned heat conduction, radiative cooling (Hildner 1974) and coronal heating assumed to be proportional to the density and to initially balance the cooling (see Choe & Lee 1992 for details and references therein).

2. CASE A: A BIPOLAR ARCADE WITH FOOTPOINT SHEAR

When the footpoints of a bipolar arcade are slowly sheared, the first stage of evolution is almost adiabatic. The shear-induced expansion decreases the plasma temperature and this adiabatic cooling primarily causes the enhancement of radiative cooling. Due to the stratification of the atmosphere, the expanding field lines pull up higher density material from below and the local density decrease in the actively expanding region is not so severe as it would be in a nonstratified atmosphere. Even a local density increase is achieved above a certain height. This upward material transport also enhances the radiative cooling. As the temperature decreases the radiative cooling becomes more and more dominant in temperature variation and a runaway cooling—thermal instability—is thus effected. At $t \approx 7500$ s a patch of plasma quickly cools down to $T \approx 10^4$ K. The resulting pressure imbalance drives material in the vicinity to the cooled region. Starting from this region, plasma cools down successively upward and downward and material is sucked in mostly by the siphon-type field-aligned flows. The condensed material thus forms a vertically extended sheet-structure, in which the maximum density is 70 times as high as the initial density. The high density material presses down the field lines to form a upwardly concave dip (Figure 1(a)), an essential signature of the Kippenhahn-Schlüter type prominences.

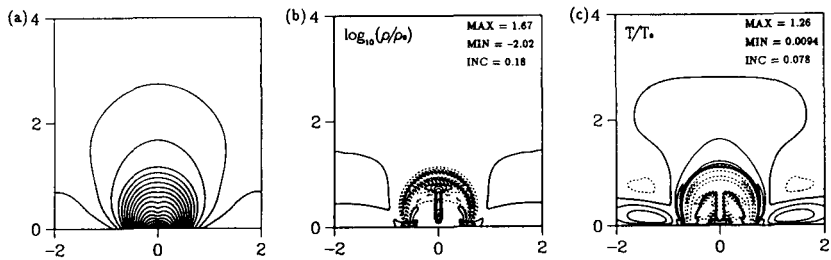

Fig. 1. Case A: Formation of a normal polarity prominence by footpoint shear. Each panel shows (a) field lines, (b) contours of the logarithm of the ratio of the density to the initial value, and (c) contours of the ratio of the temperature to the initial value. The solid line refers to increase of a quantity, the dotted line to decrease and the thick solid line to no variation. The length unit is one scale height ($\approx 6 \times 10^4$ km).

https://doi.org/10.1017/S0252921100028967 Published online by Cambridge University Press

At a higher altitude, the cooling takes place over a broader region along field lines, and above a certain height the field-aligned component of gravity overcomes the pressure gradient at the edge of the cooled plasma. The upward growth of the prominence is thus saturated and the condensed material slides down along field lines. The depletion of material results in an arc-shaped cavity of low density around the prominence (Figure 1(b) and (c)).

3. CASE B: A BIPOLAR ARCADE WITH SHEAR AND CONVERGENCE

In this case, the footpoints of a bipolar arcade are first sheared and then converged towards the neutral line. The arcade in this case is designed to have a higher curvature of field lines than that in Case A. The arcade first expands by the shear and the plasma cools down quasiadiabatically. A thermal instability also sets in, but the cooled material condenses downward along field lines without forming a prominence due to the high curvature of field lines. As the footpoints get closer by the converging motion, a current layer develops along the lower part of the vertical axis of the arcade, where magnetic reconnection takes place as in Lee (1990) and Inhester, Birn, & Hesse (1992). The highly enhanced density in the magnetic island triggers thermal instability inside the island. The cooled material condenses downward along the field lines and is finally accumulated at the bottom of the looped field lines. By successive reconnection and condensation, a sheet structure of condensed material is formed extending from the center to the bottom of the island (Figure 2(a)). The maximum density increase is 100 times the initial local value. About 92% of the mass in the island is concentrated in the prominence and the rest of the island volume constitutes a low pressure cavity (Figure 2(b)). In Case B, an *inverse polarity* prominence is attained.

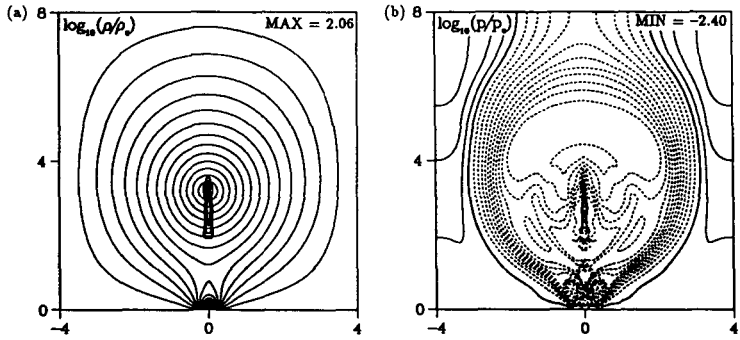

Fig. 2. Case B: Formation of an inverse polarity prominence by a shearing and converging motion. Plotted are (a) contours of density variation ($\log_{10}(\rho/\rho_0) \geq 0$) superimposed on magnetic field lines and (b) contours of pressure variation ($\log_{10}(p/p_0)$). The pressure is at minimum in the mushroom-shaped region above the prominence.

https://doi.org/10.1017/S0252921100028967 Published online by Cambridge University Press

4. Case C: TWO BIPOLAR ARCADES UNDER FOOTPOINT MOTION

In this case, two adjacent bipolar regions are mimicked by a quadrupolar field initially without an X-point (Low 1992). On the footpoint level, we give a shear and a slower converging motion. By the shear both arcades expand separately and expel flux towards each other. A current layer is thus formed starting from the neutral line, where the first magnetic reconnection takes place. The X-point slowly rises in time with successive reconnection of field lines. As in the previous cases, the expansion of arcades induce the quasiadiabatic temperature drop except near and below the X-point. The local density is decreased within the two expanding arcades except near the X-point, but increased in the overlying arcade. This density enhancement is mainly attributed to the material outflow from the reconnection region. The sudden cooling to the chromospheric temperature first takes place in the overlying arcade. The successive condensation upward and downward results in a vertical sheet structure of the prominence (Figure 3). Different from Case A, no shedding of condensed material can be seen owing to the rather flat field geometry. In this case, we have another type of *normal polarity* prominence. The low plasma β (≤ 0.01) tells that the dips on field lines are not caused by the gravity of high mass but by the intrinsic field geometry.

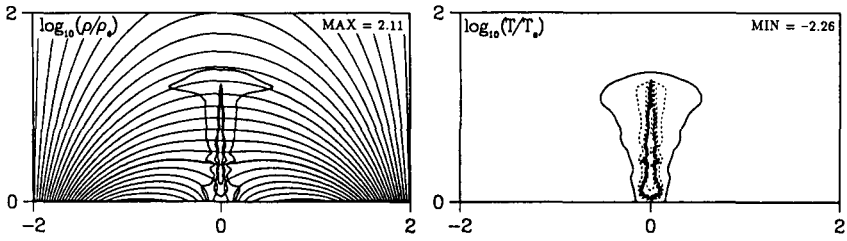

Fig. 3. Case C: Formation of a normal polarity prominence between two bipolar arcades. Plotted are contours of density variation ($\log_{10}(\rho/\rho_0) \geq 0$) superimposed on field lines and contours of temperature variation ($\log_{10}(T/T_0) \leq 0$).

5. DISCUSSION

The mechanism of prominence formation in Case A is restricted by the density and the plasma β. The condensation cannot be achieved within a reasonable time if the density at the coronal base is far less than $10^9\,\mathrm{cm}^{-3}$, and a dip on field lines is hard to form if $\beta < 0.1$ (Lee, Choe, & Akasofu 1992). But the β-restriction can be relaxed with an increasing magnetic shear. This mechanism may thus be applied to low-lying filaments in active regions where the density is higher than in quiet regions. In this respect, it is noteworthy that

https://doi.org/10.1017/S0252921100028967 Published online by Cambridge University Press

normal polarity prominences are usually located lower than inverse polarity prominences (Leroy 1989).

Mechanisms B and C are free from the β-restiction. Although the linear cooling time-scale indeed depends on the initial density, the magnetic reconnection can efficiently enhance the local density. Furthermore, the effect of heat conduction is minimized in Mechanism B. In the aspect of stability, the prominence in Case B seems to be most stable to the lateral perturbation. The high location of the prominence in Case B is consistent with the aforementioned statistics. This prominence model is thus close to the long-lived quiet region prominences.

The peculiar field geometry in Case C allows this mechanism to work with most diverse flow patterns. Due to the existence of an X-point, a weak field corridor is naturally realized, and a high shear angle of photospheric magnetic fields can be readily obtained with a small amount of footpoint shear. Our model prominence in Case C shows a normal polarity geometry at a modest height and thus resembles a low-lying active region filament. However, we cannot exclude the possibility of transition to a field geometry with an island either by a secondary reconnection at a high altitude or by a multiple X-line reconnection (Lee & Fu 1986) in a long current sheet.

ACKNOWLEDGEMENT

This work was supported by DOE grant DE-FG06-89ER 13530 to the University of Alaska.

REFERENCES

Choe, G. S. & Lee, L. C. 1992, *Solar Phys.* **138**, 291
Hildner, E. 1974, *Solar Phys.* **35**, 123
Inhester, B., Birn, J., & Hesse, M. 1992, *Solar phys.* **138**, 257
Kippenhahn, R. & Schlüter, A. 1957, *Zs. Ap.* **43**, 36
Kuperus, M. & Raadu, M. A. 1974, *Astr. Ap.* **31**, 185
Lee, L. C. 1990, a presentation given in the 'Workshop on Solar Flares and Magnetospheric Substorms', Hawaii (unpublished)
Lee, L. C., Choe, G. S., & Akasofu, S.-I. 1992, in M. Ashour-Abdalla & T. Chang (eds.), *Micro/Meso Scale Phenomena in Space Plasmas*, AGU, Washington, D.C. (in press)
Lee, L. C. & Fu, Z. F. 1986, *J. Geophys. Res.* **91**, 6807
Leroy, J. L. 1989, in E. R. Priest (ed.), *Dynamics and Structure of Quiescent Solar Prominences*, Kluwer Academic Publishers, Dordrecht, Holland, p. 77
Low, B. C. 1992, *Astr. Ap.* **253**, 311
Martin, S. F. 1990, in V. Ruždjak & E. Tandberg-Hanssen (eds.), *Dynamics of Quiescent Prominences*, IAU Colloquium 117, Springer-Verlag, Berlin, p. 1
Rompolt, B. & Bogdan, T. 1986, in A. Poland (ed.), *Coronal and Prominence Plasmas*, NASA Conference Publication 2442, Washington, D.C., p. 81
Tang, F. 1987, *Solar Phys.* **107**, 233